AMERICAN UNIVERSITY OF BEIRUT



COAXIAL PERSONALIZED VENTILATION SYSTEM AND
WINDOW PERFORMANCE FOR HUMAN THERMAL
COMFORT IN ASYMMETRICAL ENVIRONMENT



by
SYLVIE JACQUES ANTOUN



A thesis
submitted in partial fulfillment of the requirements
for the degree of Master of Engineering
to the Department of Mechanical Engineering
of the Faculty of Engineering and Architecture
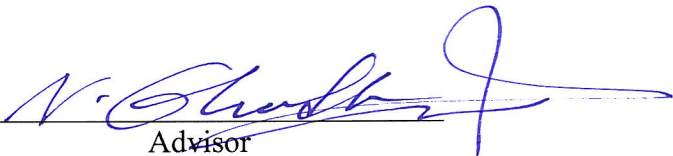at the American University of Beirut



Beirut, Lebanon
July 2015

AMERICAN UNIVERSITY OF BEIRUT

# COAXIAL PERSONALIZED VENTILATION SYSTEM AND WINDOW PERFORMANCE FOR HUMAN THERMAL COMFORT IN ASYMMETRICAL ENVIRONMENT

by
SYLVIE JACQUES ANTOUN

Approved by:

_____

Dr. Nesreen Ghaddar, Professor                    Advisor
Department of Mechanical Engineering, AUB


_____

Dr. Kamel Ghali, Professor                    Member of Committee
Department of Mechanical Engineering, AUB


_____

Dr. Fadl Moukalled, Professor                    Member of Committee
Department of Mechanical Engineering, AUB


Date of thesis/dissertation defense: July 20, 2015

# AMERICAN UNIVERSITY OF BEIRUT

# THESIS, DISSERTATION, PROJECT RELEASE FORM

Student Name: ___Antoun_____Sylvie_____Jacques_____

                          Last              First             Middle

● Master's Thesis         ○ Master's Project         ○ Doctoral   Dissertation

[✓]     I authorize the American University of Beirut to: (a) reproduce hard or electronic copies of my thesis, dissertation, or project; (b) include such copies in the archives and digital repositories of the University; and (c) make freely available such copies to third parties for research or educational purposes.

[ ]     I authorize the American University of Beirut, **three years after the date of submitting my thesis, dissertation, or project,** to: (a) reproduce hard or electronic copies of it; (b) include such copies in the archives and digital repositories of the University; and (c) make freely available such copies to third parties for research or educational purposes.

_____     August 4, 2015_____

Signature                         Date

# ACKNOWLEDGMENTS

Scientific research requires a lot of commitment of both time and effort to come up with a successful research work. Therefore, this thesis work is not the fruit of an individual effort and it could not have been achieved without the support and assistance of many persons. For that reason, I would like to thank a few.

I would like to thank my advisors at the American University of Beirut for their continuous support and guidance throughout my research work. I acknowledge the effort of Dr. Nesreen Ghaddar and Dr. Kamel Ghali for their original involvement and guidance, and motivation which contributed a lot to this thesis.

I would like also to thank my committee member, Dr. Fadl Moukalled for his attendance and guidance especially in the numerical simulations. I would like to thank all staff and faculty members of the American University of Beirut for their great help and patience, which contributed a lot to the smooth achievement of my thesis.

I would like to express cordial gratitude to my friends and colleagues at the American University of Beirut who without them I would not have been able to achieve what I have reached in particular Rachid Idriss, Nagham Ismail, Carine Habchi, Bachir el Fil and Walid Abou Hweijj.

Also I express great thanks to my dearest friends and family (Father, Mother, and my sisters) for their patience and continuous unconditional support.

# AN ABSTRACT OF THE THESIS OF

Sylvie Jacques Antoun    for        Master of Engineering
Major: Mechanical Engineering

Title: Coaxial Personalized Ventilation System and Window Performance for Human Thermal Comfort in asymmetrical environment

This paper assesses the energy performance and occupant comfort of a ceiling mounted coaxial personalized ventilation system in presence of radiation asymmetry due to a large window for different glazing systems.  Detailed 3-D computational fluid dynamics (CFD) simulations were performed to study the flow and thermal fields in the conditioned office space and evaluate longwave and diffuse shortwave radiation effect on the occupant seated directly below the PV nozzle. The CFD model was coupled to a bioheat model to predict the corresponding local and overall thermal comfort of human body parts subject to the asymmetrical environment. The CFD model is validated by conducting experiments in a climatic room equipped with the PV system and using a thermal manikin facing a hot surface. Predicted and measured values of segmental skin and air temperature at the vicinity of the thermal manikin are compared. Good agreement (less than 8% error) was found between the measured and predicted values.

Extensive simulations were performed to evaluate the effect of different types of window glazing on the perceived thermal comfort under various PV operating parameters. For high performance window, the energy performance of the coaxial PV system was compared to mixing ventilation system. Remarkable energy savings up to 36% were achieved at the same level of thermal comfort and environmental outdoor conditions.

# CONTENTS

# LIST OF ILLUSTRATIONS

# LIST OF TABLES

# CHAPTER 1

# INTRODUCTION

Large glazing facades are catching on in the workspaces faster than ever. They improve building aesthetic appearance and remedy the bomb-shelter syndrome in offices by allowing natural lighting, creating bright and productive spaces conductive to modern work styles. When an occupant is sitting near a glazed surface, shortwave and longwave radiation asymmetry can influence human thermal comfort [1,2]. During summer conditions, it is important to mitigate the unpleasant impact of solar radiation on occupant's thermal comfort and reduce the cooling loads and energy costs. The impact of solar radiation on window performance is determined by the window optical properties and it is divided into two components: transmitted solar radiation and absorbed radiation [1,2]. The transmitted radiation controls how much shortwave radiation reaches the body while the absorbed radiation controls how much the window temperature will increase and cause radiation asymmetry for the occupant. These radiant heating effects act on the human body asymmetrically, causing some body segments to be considerably warmer and sensitive to local skin temperature and discomfort caused by windows.

The relation between the effect of windows (glazing and shading devices) on indoor conditions and energy consumption has been widely explored especially in office buildings. Tsikaloudaki et al. [3] studied the cooling energy performance of windows with respect to their thermal and optical characteristics. Hwang and Shu [4] evaluated the effect of different types of glass building envelope on both thermal comfort and

1

energy saving potential. Similarly, Cappelletti et al. [5] evaluated the energy glazing performance by maintaining fixed comfort conditions and calculating the Predicted Mean Vote (PMV), taking into account the effect of the solar radiation. In addition, Huizenga et al. [1] assessed the window performance on human thermal comfort for different fenestration systems (various combinations of solar heat gain coefficient, U-value, solar transmittance, window areas and frames, view factors and incident radiation). They concluded that new high performance windows can alleviate thermal discomfort by reducing the effect of radiation asymmetry, solar heat gain and cooling costs during summer season.

Different heating, ventilation, and air conditioning (HVAC) systems have different energy requirements to provide indoor environmental conditions for occupant comfort and air quality needs. Most offices and residential buildings are air conditioned with conventional HVAC systems which maintain the space at a uniform temperature and indoor air quality through mixing. The mixing air distribution system controls the entire space at a fixed air temperature regardless of space occupation. However, such systems can create thermal tension in highly glazed spaces and fail to satisfy thermal comfort needs [6, 7]. A person sitting near a window would feel warm and prefer a lower thermostat temperature; while the other person sitting away from the window would feel cool and desire a higher thermostat temperature, thus a conflict of thermal preferences would occur. Finally, mixing systems will require higher energy consumption when delivering cool air to a partially occupied open space to provide a uniform temperature and homogenous indoor air quality [8,9]. Most of the studies of window performance on

thermal comfort and energy savings were conducted for conventional mixing system applications.

In harsh hot climates like in the Gulf region, the use of high performance window might mitigate the effect of transmitted solar radiation and reduce human discomfort. However, it might not be energy efficient when combined with mixing systems and compared to localized air conditioning systems such as the coaxial PV system that delivers fresh cool air directly to the breathing zone. Halvonova & Melikov [10, 11] suggested desk-mounted personalized ventilators (PV) with adjustable supply air flow rates and temperatures which allow the occupant to control his/her own microclimate and attain a desirable thermal comfort. Displacement ventilation systems are generally combined with the PV systems; they contribute in the supply and transport of fresh air to the PV modules through individual ducting or using ductless systems close to the floor. On the other hand, Yang [12,13] proposed the integration of the PV device with a mixing ventilation system using a ceiling-mounted PV for offices in tropical climates, thus eliminating the need to extend ducting system of the task ventilators into the occupied zone. The PV delivers fresh air while the peripheral diffusers supplies recirculated air. Yang came up with a 5% energy savings to cool an occupant seated directly under a PV nozzle supplying fresh air at 4.5L/s when compared to a mixing system delivering the same amount of fresh air and maintaining the average room temperature of 23.5 °C [13].

Makhoul et al. [14] proposed a PV system corresponding of a ceiling-mounted coaxial PV nozzle integrated with a peripheral diffuser capable of localizing thermal comfort needs. The main advantage of the coaxial PV nozzle is that it reduces the entrainment

between the clean air and the return air, thus it provides better indoor air quality (IAQ) at a reduced clean airflow rate and an acceptable localized thermal comfort state, while the peripheral diffuser help creating a canopy of conditioned air around the human body and an isolated environment in an open office via a localized airflow. Makhoul investigated the ventilation effectiveness of the proposed system and deduced that coaxial nozzle was able to achieve three to four times better ventilation effectiveness when compared to single jet PV system. On the other hand, Makhoul et al. [15] studied the energy performance of the proposed system with regard to its ability to provide thermal comfort and 34% of energy savings was achieved when compared to conventional mixing systems. The main advantage of Makhoul's system is that it allows occupants to control their own microclimates according to their needs by varying the coaxial PV flow rates. The coaxial personalized ventilator might offer an efficient air conditioning system in the case of radiant asymmetry. Therefore it would be important to consider the interaction of both glazing and coaxial PV system performance.

In many studies, the effect of diffuse radiation was accounted as an increase in the window surface temperature [1]. However, this method cannot be adopted in non-homogeneous conditions problems such as with ceiling mounted personalized ventilation systems. The coaxial PV system creates non-homogeneous thermal condition, and the employment of large window can disturb the flow field and thermal comfort through longwave and shortwave radiation. Consequently, the fluid dynamics, temperature distribution and solar radiation load associated with the coaxial PV system become very complex to detect. Thus, CFD simulations are required to accurately model the flow inside the office. To predict human comfort state, a thermal bioheat and

4

local thermal comfort models should be integrated with the CFD model. Since a localized air conditioning system was tested and radiation asymmetry is a new a factor, local thermal comfort and local sensation need to be reassessed for PV performance under asymmetric radiation.

In this study, the bioheat model of Salloum et al. [16] integrated with the thermal comfort of Zhang [17-20] is adopted. The bioheat consisted of a multi- node model of 15 body segments that calculates segmental skin temperatures whereas the thermal comfort model allows the estimation of the segmental comfort of the occupant under non-uniform environmental conditions based on an 8-point scale of sensation and comfort [21, 22]. The validation of the CFD predictions coupled with the bioheat and comfort models will be done by experiments on thermal manikin. This will be followed by a parametric study to evaluate different window glazing systems and supply diffuser flow rate on thermal comfort and energy consumption. Finally, the performance of the PV system, in terms of energy savings, was compared to a conventional mixing ventilation system at nearly equal comfort using same window type, room design and outdoor conditions.

# CHAPTER 2

# SYSTEM DESCRIPTION

The system proposed by Makhoul [14, 15], a coaxial ceiling mounted personalized ventilator, is considered in our study. It consists of supplying cool fresh air at specific temperature and flow rates in order to provide the desirable conditions for thermal comfort and indoor air quality (IAQ). The air distribution system composition consists of: (i) a primary nozzle that delivers cool fresh air, a secondary annular nozzle that delivers recirculated air and reduces shear and mixing effect by bordering the fresh air core region [14]; (ii) a peripheral angled diffuser that delivers recirculated air at a 45° angle to form a canopy for localizing the flow around the occupant and maintain the room macroclimate temperature. Equal velocities were maintained at the outlet of the primary and secondary jet in order to reduce the mixing at the jets' interface and extend the downward distance travelled by the fresh air primary core nozzle.

The ceiling mounted coaxial PV nozzle was centered over the occupant's head which was facing a glazed facade exposed to the outdoor summer conditions. The distance between the window and occupant was fixed at 1m considering it to be a critical distance for radiation asymmetry and thermal comfort [1]. The heat load inside the office was generated by internal heat gains such as thermal manikin (39 $W/m^2$), lighting (10 $W/m^2$) and desktop computer (93 W) [14, 23] in addition to solar radiation heat gain coming from the window. Note that solar thermal load depends on the glass size and optical properties (energy absorptivity, transmissivity and reflectivity) and the solar radiation intensity striking the window.

# CHAPTER 3

# METHODOLOGY

The objective of this study is to assess thermal comfort of an occupant exposed to solar radiation effect from different glazing systems and air conditioned by a coaxial PV system. This will be followed by a comparison of the effectiveness of the proposed system with a conventional mixing ventilation system at nearly equal comfort, same room design and extreme hot conditions. To assess the effect of radiation asymmetry from a hot window and the energy performance of the coaxial PV system in providing localized thermal comfort, 3-D detailed numerical simulations combined with a radiation model were performed using commercial software such as ANSYS Fluent [24]. To study the thermal comfort effect of the coaxial nozzle operating conditions (supply flow rate, return and fresh air temperatures), the bioheat model of Salloum et al. [16] and the comfort models of Zhang et al. [17-20] were integrated with the CFD code to predict the human thermal response and segmental and overall thermal sensation and comfort. An experimental setup was conducted in order to validate the CFD model. The validated numerical models were then used to perform a parametric study to determine best combination performance of window type and system operating parameters (jets flow rates, temperatures, glazing optical properties).

## 3.1 Airflow Modeling

The commercial CFD solver, ANSYS Fluent [24] is used to solve numerically for the air velocity and temperature fields. We used a symmetry plane passing through the

7

center of the manikin, nozzles, and window and dividing the room to one-half when numerically modeled through a grid as shown in Fig.1. The Navier-Stokes and energy equations used by Fluent [24]:

$$\frac{\partial \rho}{\partial t} + \nabla.\left(\rho \vec{v}\right) = 0$$

$$\rho \frac{D\vec{v}}{Dt} = -\nabla p + \nabla \cdot \mathrm{T} + \mathrm{f}$$

$$\frac{\partial}{\partial t}\left(\rho E\right) + \nabla.\left(\left(\rho E + p\right)\vec{v}\right) = \nabla.\left(k\nabla T - \sum_j h_j \vec{J}_j + \left(\mathrm{T}.\vec{v}\right)\right)$$

Eq. (1) represents the continuity equation that allows accounting for the density variation inside the space and mass conservation. Eq. (2) indicates the momentum equation for the modeling of the flow dynamics in the computational domain. It relates the inertia term on the left-hand-side to the pressure gradient $\left(-\nabla p\right)$, the shear stress term $\left(\nabla.\mathrm{T}\right)$, and the body forces term $\left(\mathrm{f}\right)$. Eq. (3) represents the energy equation that relates the convective heat transfer on the left-hand-side to the energy transfer due to conduction $\left(k\nabla T\right)$, species diffusion $\left(\sum_j h_j \vec{J}_j\right)$, and viscous dissipation $\left(\mathrm{T}.\vec{v}\right)$.

In order to capture the entrainment process with jet deflections between the fresh air jet and the recirculated air from the surrounding nozzles, a tetrahedral unstructured grid was produced using different element sizing for the boundary faces. In addition, four spheres of influence of 1m diameter were integrated between the nozzles in the ceiling and the thermal manikin and the grid was clustered in this region and unstructured in the rest of the domain as shown in Fig.1. An inflation boundary layer was created at the

walls and manikin's surface of smooth transition type, with a growth rate of 1.2 and a total number of 3 layers. The reason of adding the inflation is to accurately capture the boundary layer region for any wall-bounded turbulent flows. The corresponding y+ values ranged between 0.8 and 4 [14,15,24].
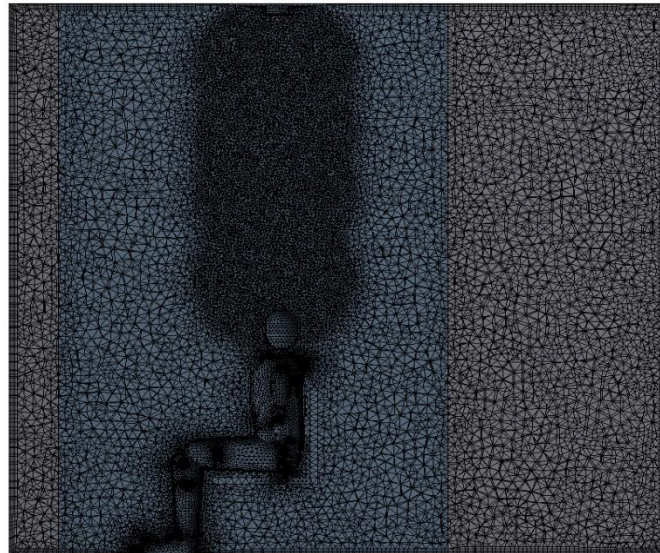


**Fig. 1 Grid generated at symmetry plane**

A grid independency was performed in order to reduce the computational time and the number of cells while guaranteeing that the current mesh used is fine enough to generate accurate results. The resolution of the mesh in the critical regions was refined until the radiant and air temperature at the vicinity of the thermal manikin (chosen as the criteria for the test) was stabilized. As shown in Fig. 1, a grid system with different grid sizing and number of cells were generated, and used to perform a test simulation. The finer grid consisted of 2,439,819 while the coarser grid consisted of 781,524 cells. The results showed that the grid of 1,424,478 elements is the best to be considered for the final simulations.

The realizable k-ε turbulence model is used to predict the spreading rate of planar and round jets and its suitability for modeling recirculation in ventilated rooms; the k-ε RNG model is used for the turbulence modeling. This is because the model is effective for both high and low Re number turbulent flows and therefore it can produce good quality results even for the situations when the flow is not fully turbulent. Enhanced wall treatment is applied to the walls for better adaptation of the turbulence model. Besides, the incompressible ideal gas law will be selected for the density to account for buoyancy effects. The turbulence kinetic energy and dissipation rate and the momentum equations are discretized using a second-order upwind scheme. In addition, the "PRESTO!" scheme is applied for the pressure.

**3.2 Radiation Solar Model**

According to Huizenga and Hoffman [1, 26], direct radiation that hits the occupant on sensitive body parts such as the head automatically leads to a perception of the room conditions as very uncomfortably hot. Therefore, we can assume that occupant will mitigate the discomfort due to direct solar radiation by relocating or adjusting blinds or shades [1, 27]. In our analysis, the investigation of radiant heating through the window was due to the amount of transmitted diffuse solar radiation (shortwave radiation) absorbed by the body (or clothing) and asymmetric radiation fields caused by long wave radiation exchange with the high interior surface temperature of the glazing[1]. The airflow and temperature distribution inside the room are highly influenced by the outdoors conditions: for example shortwave and longwave radiation affect indirectly the flow field and consequently thermal comfort by increasing the air and surface temperatures of the space.

Different radiation models are presented in ANSYS/Fluent [24, 25]. In this study, the solar load model adopted in Fluent consisted of a combination of the S2S model and the solar ray tracing algorithm [28-31]. The solar ray tracing calculates the radiation effects from the sun that enter the computational domain. It accounts for the shortwave radiation by specifying the diffuse solar radiation incident on a surface (note that direct solar irradiation was set to zero). Nevertheless, the solar load model does not deal with emission from surfaces. Therefore, the surface-to-surface (S2S) radiation model was used to compute longwave radiation heat exchange between the surfaces in the workspace. The main advantage of the S2S is that it does not account for participating medium (air is transparent). The surfaces were assumed to be gray with specified emissivity as shown in Table 2 [24, 25]. To evaluate the influence of different window type on thermal comfort and energy consumption, four different kinds of glazing systems were investigated and classified from low to high performance with the features indicated in Table 1 [1, 32]. Making sure of reaching numerical convergence is an important and crucial step towards obtaining reliable and conclusive results. The convergence was judged when the normalized residuals of flow equations were less than $10^{-4}$, the energy and radiation equations were less than $10^{-6}$, and the net heat flux of the computational domain was below 1% of the total heat gain. Under-relaxation factors 0.3, 0.7, 0.3, 0.8, 0.8, 0.8, 0.9 for pressure, density, momentum, turbulent kinetic energy, turbulent dissipation rate, turbulent viscosity, energy respectively were used. [14, 15, 24].

**Table 1**

**Glazing generic Systems Properties**

| CODE | EQUIVALENT GLAZING SYSTEM | SOLAR ENERGY | | | $k_{eff}$ |
| | | $\tau_{sol}$ | $\alpha_{sol}$ | SHGC | [W/(m$^2$K)] |
|------|---------------------------|--------------|----------------|------|-------------|
| G1 | Clear double glazing, 0.027m | 0.61 | 0.28 | 0.70 | 0.19 |
| G2 | Low-ε double glazing, 0.027m | 0.51 | 0.31 | 0.62 | 0.07 |
| G3 | Low-ε triple glazing, 0.05m | 0.38 | 0.41 | 0.51 | 0.09 |
| G4 | Spectrally selective low-triple glazing, 0.05m | 0.27 | 0.42 | 0.36 | 0.08 |

## 3.3 CFD, Bioheat and Comfort Models Coupling

To accurately regulate flow and thermal parameters of the coaxial jet nozzle and incorporate long wave and solar load radiation effects, the bioheat model of Salloum et al. [16] and the comfort models of Zhang et al. [17-20] were integrated with the CFD code. The bioheat model was coupled with the CFD simulation through data exchange of radiant and air temperatures and velocity in order to resolve the thermal and air flow interactions between the human subject and his environment. This coupling allowed us to predict the human segmental skin temperatures and heat flux conditions for the CFD model and assess occupants segmental and overall body thermal comfort [16]. The bioheat model divides the body into 11 segments (head, chest, back, abdomen, buttocks, upper arm, lower arm, hands, thighs, calves and feet to simulate the physiological

responses of each body segment for predicting later its state of thermal comfort based on Zhang's model in a high transient thermal environment. Zhang's model permits to predict an 8 point scale thermal sensation and thermal comfort while taking into account the transient variation of the skin and core temperatures [17-20]. This would make the model more robust when accounting for local segmental comfort in transient conditions. The local or segmental sensation is a function of local skin, mean-skin and core temperatures and their rates of change [33]. The local- and mean-skin temperatures represent the response to stable conditions, and the derivatives of skin temperature and core temperature represent response to transients as is described by Eq. (4):

$$\text{Local Sensation} = f\left( T_{skin,i}, \frac{\mathrm{d}T_{skin,i}}{\mathrm{d}t}, \overline{T_{skin}}, \frac{\mathrm{d}T_{core}}{\mathrm{d}t} \right)$$

The temperatures and velocities obtained from Fluent were used as inputs to the bioheat model to update the skin temperatures. This procedure was repeated until the manikin skin temperature no longer varies along with the converged solution of the temperature field. The above coupling procedure can be summarized in Fig. 2.
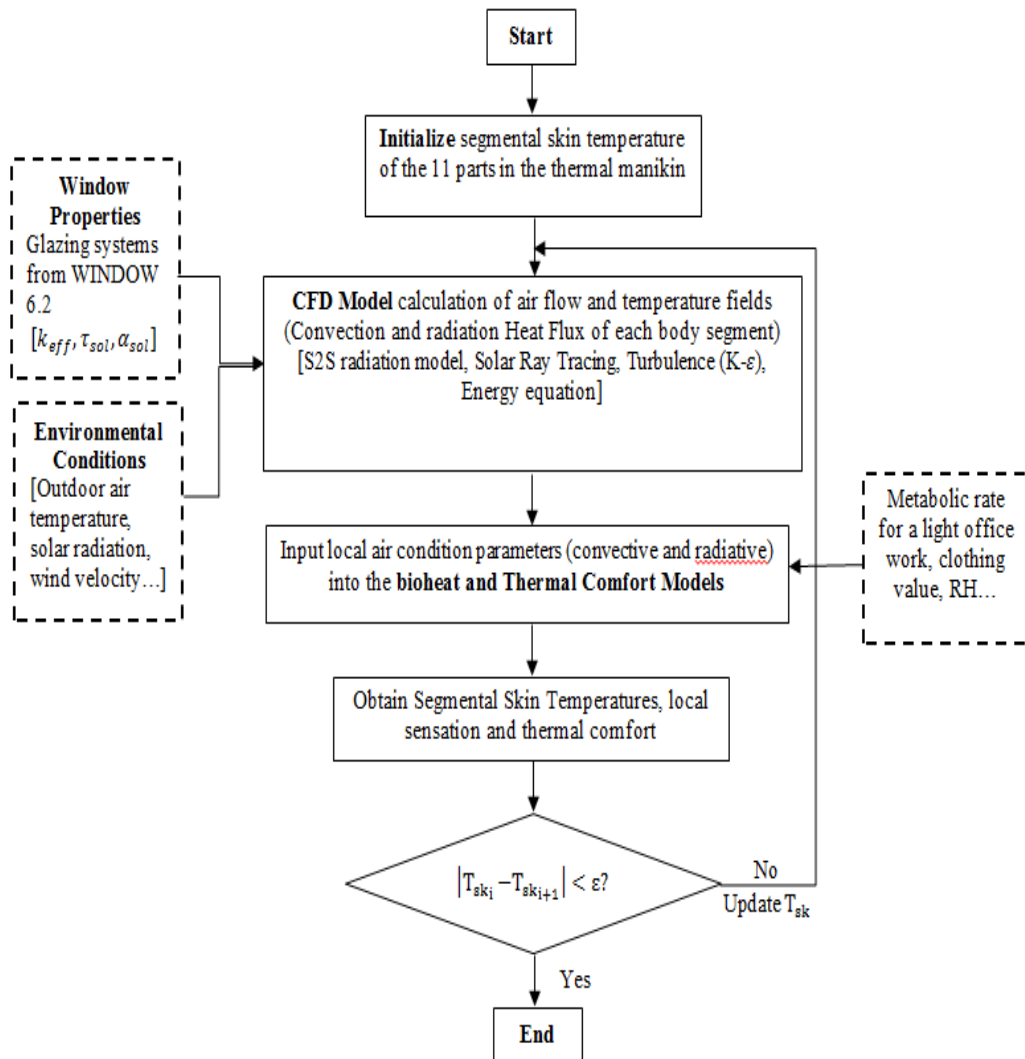
**Fig. 2 Simulation models diagram**

## 3.4 Experimental Setup

The performance evaluation of the coaxial personalized ventilation system performance and the effect of radiation asymmetry due to longwave radiation of an occupant were validated by experiments on a thermal manikin seated close to a window performing in a climatic chamber as shown in Fig. 3.

The objective of our experiment is to validate the capability of the CFD model of capturing the physics of radiation asymmetry due to long wave radiation exchange with a hot surface and make sure that occupant interaction with the surroundings are properly modeled. The experimentation assessed thermal field variation inside the chamber and thermal manikin skin temperature response when exposed to different level of radiation asymmetry due to various surface panels' temperature. In order to provide accurate boundary conditions for the CFD model, additional measurements of the flow characteristics at the outlet of the PV nozzles were conducted during the experiment.
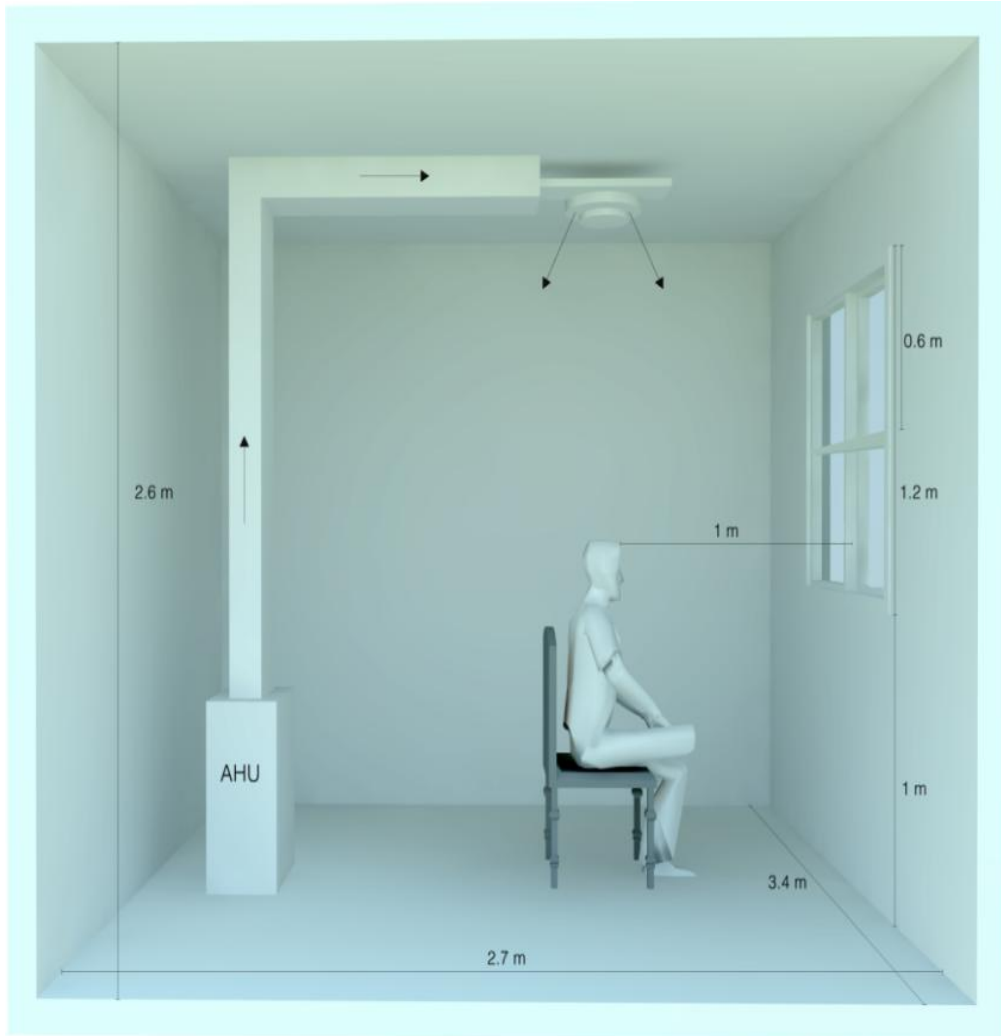
**Fig. 3 Schematic of the conditioned space**
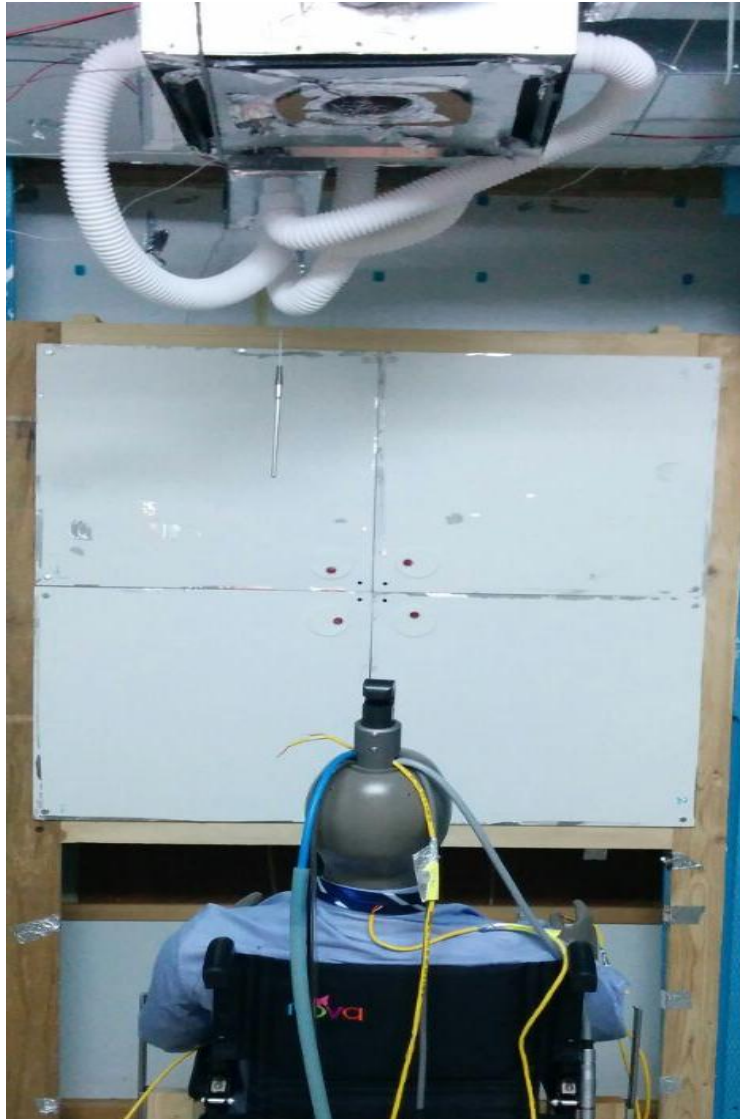
In the experiment, the diffuse radiation was not included and only radiation asymmetry due to longwave radiation exchange between occupant and the hot surface was tested. According to Sabine Hoffmann et al [26], the transmitted diffuse radiation falling on the occupant is uniformly distributed on the body, thus it increases the local sensation of all body parts to a similar degree and results in an overall warm sensation while the overall comfort can still be acceptable. Therefore, the transmitted diffuse radiation is not a factor of the radiation asymmetry and it is simply a distributed load on the body parts that will create an overall warm sensation [26].

**Table 2**

**Solar radiation model and boundary conditions**

| Solar radiation model | |
|---|---|
| Solar radiation algorithm | Solar ray tracing algorithm |
| Radiation model | Surface-to-surface (S2S) model including view factors |
| Diffuse solar irradiation | 300 W/m$^2$ |

| Boundary conditions | |
|---|---|
| Thermal manikin | Constant surface temperature |
| Coaxial nozzles and Diffuser | Velocity-inlet, internal emissivity $\varepsilon = 1$ |
| Window | Convective, semi-transparent wall with shell conduction, internal emissivity $\varepsilon = 0.84$ |
| Ceiling | Constant heat flux, opaque wall, internal emissivity $\varepsilon = 0.9$ |
| Partition Walls, floor and | Adiabatic, opaque walls, internal emissivity $\varepsilon = 0.9$ |

## 3.5 Experimental Protocol and Measurements

The experimental validation process took place in a climate chamber (3.4 m × 2.7 m × 2.6 m) constructed of highly insulated walls and an internal layout of a typical office. Four electric panel heaters were installed at the central location of the wall as seen in

Fig. 3. Each panel had dimensions of 0.6 m × 0.6 m and a maximum power of 400 W, together they represented a 1.2 m × 1.2 m hot window placed 1m above the floor and emitting longwave radiation with the surroundings. The surface temperature of the panels was controlled by the panel power input, which was adjusted using a proportional accurate controller that permits programming resistor power according to desired value. An epoxy thermal manikin "Newton" mimicking a human being was seated on a chair directly below the coaxial PV nozzle and positioned 1 m away from the radiant heating panels along the centerline of the their total surface. "Newton" was manufactured by Northwestern Measured Technology and consisted of 20 independently controlled thermal zones connected to the thermal manikin software that reported: segmental comfort and sensation, local skin temperatures, and generated heat flux [34]. The thermal manikin was dressed of typical office clothing: a long sleeved shirt and pants such that the overall resistance is 0.6 clo. The cooling load into the space was mainly due to internal loads such as lighting ($10W/m^2$), the thermal manikin (70 W) in addition to heat load generated by the hot surface panels.

The air conditioning of the space was served by two Honeywell (2.64 kW) air-handling units: one conditioning the recirculated air and the other supplies conditioned fresh air. Peripheral ceiling diffusers and secondary nozzle of the coaxial PV were supplied from a recirculation air handling-unit and the primary nozzle of the coaxial PV was supplied from the fresh air-handling unit. The air temperatures and flow rates were controlled by installed dampers and in-flow electric heaters. To reduce the flow turbulence intensity and airflow mixing the primary nozzle was fitted with honeycomb flow straighteners and two screens. The setup allows for variations in the panels surface temperature while

maintaining the coaxial PV operating conditions fixed. Prior to each set of measurements, the manikin was initialized to its neutral set point and the PV system was turned on for at least 3-4h in order to reach steady state conditions.

In order to validate the thermal flow field and monitor its variation at the vicinity of the thermal manikin, a set of 11 K-type thermocouples with an accuracy of ± 0.5 °C were distributed along the different segmental body parts (see Fig. 4). These thermocouples were connected to an OMEGA DaqPro Data logger to store the data. The temperature readings were recorded at steady state (within an error of ± 0.5 °C). For temperature field validation, measurements at 11 points located around the thermal manikin were performed according to the schematic Fig.4. On the other hand, the velocity and turbulence intensity were measured at the vicinity of the nozzles using omni-directional hot-wire anemometers manufactured by TSI having a ± 3% accuracy and calibrated for low velocity range measurements (<2 m/s). These flow measurements served as boundary conditions for the PV nozzles in the CFD model.

For the model validation process, the thermal manikin underwent three experiments for which the panels' surface temperature was varied between 40 °C, 45 °C and 50 °C. These temperature values can be reachable in extreme hot regions [1]. They were selected in order to investigate the effect of a hot surface (by longwave radiation) on the thermal field surrounding the manikin. The coaxial PV operating conditions maintained in the experiment, were the following: the fresh air delivered from the primary nozzle was fixed at 16 °C and supplied at a flow rate of 10 L/s, while the recirculated conditioned air delivered from the peripheral diffuser was maintained at 16 °C at a total flow rate of 50 L/s. Note that the secondary nozzle delivered recirculated air at the

macroclimate temperature (which is considered the temperature of the air away from the human microclimate). The experimental PV supply conditions were selected according to the values used by Makhoul and proven to be effective for IAQ and thermal comfort [14, 15].
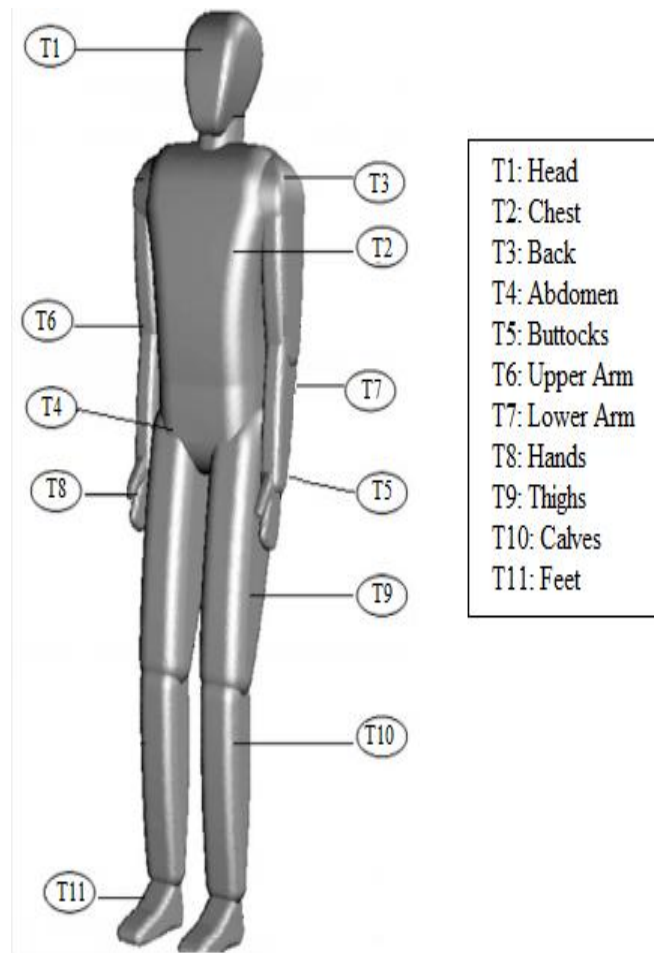


**Fig. 4 Thermocouples distribution over the manikin body parts**

## 3.6 Parametric Study

In order to assess the performance of the coaxial PV system in bringing thermal comfort to human body when it is located close to a window, a parametric study was conducted. The numerical simulations were performed under fixed steady-state outdoor climatic conditions with ambient temperature of 45 °C and diffuse radiation of 300 W/m2 at 12:30 h on July 21, 2010 which represents the peak summer time for the Gulf region [35]. These outdoor conditions were considered in all simulations. In this study, four different types of window glazing ranging from low to high-performance glazing systems were tested in order to assess the performance of the coaxial PV system and thermal comfort when radiation asymmetry and transmitted diffuse radiation vary for different level of glazing system. Table 1, as presented earlier, lists the properties of 4 glazing systems with features that are close to two double glazing and two triple glazing systems. They ranged from low to high performance windows according to their solar transmissivity, absorptivity and thermal conductivity [1,32]. A fully glazed window of 3.4 m × 2.6 m surface area was considered for all simulations and a fixed distance of 1 m between the thermal manikin and window. Each glazing system was specified with an effective thermal conductivity and an overall thickness (see Table 1). The window was set as a semi-transparent wall with an emissivity of 0.84 [1,32], while other wall boundary conditions were set as opaque walls with an emissivity of 0.9.

The primary nozzle operating conditions were fixed for all simulations at a flow rate of 8.5 L/s (according to the recommendations of ASHRAE standards 62.1-2013 [23]) and a supply temperature of 16 °C. The peripheral diffuser flow parameters were varied for

two different flow rates (50 L/s, 55 L/s) along with three different temperatures (16 °C, 18 °C, 19 °C). The secondary nozzle was at the same velocity as the primary PV nozzle and the same temperature as the peripheral diffuser. A convective boundary condition with shell conduction and a corresponding specified thickness were used for the window glass. Shell conduction option was used to apply the appropriate thermal resistance across the window thickness and calculate heat conduction without the need to mesh the window thickness in a preprocessor [24, 25]. The outdoor ambient air temperature was set to 45 °C and the external convective heat transfer coefficient was set to 21 W/m2.K using the Palyvos correlation for windward surfaces in buildings [36]. A constant heat flux of 10 W/m2 was applied to the ceiling representing the lighting load in the office (according to the recommendations of ASHRAE standard 62.1-2013 [23]). The internal load such as the desktop (93 W) was distributed on the partition walls as constant heat flux of 4 W/m2, while an adiabatic thermal condition was assumed for all other surfaces.

# CHAPTER 4

# RESULTS AND DISCUSSION

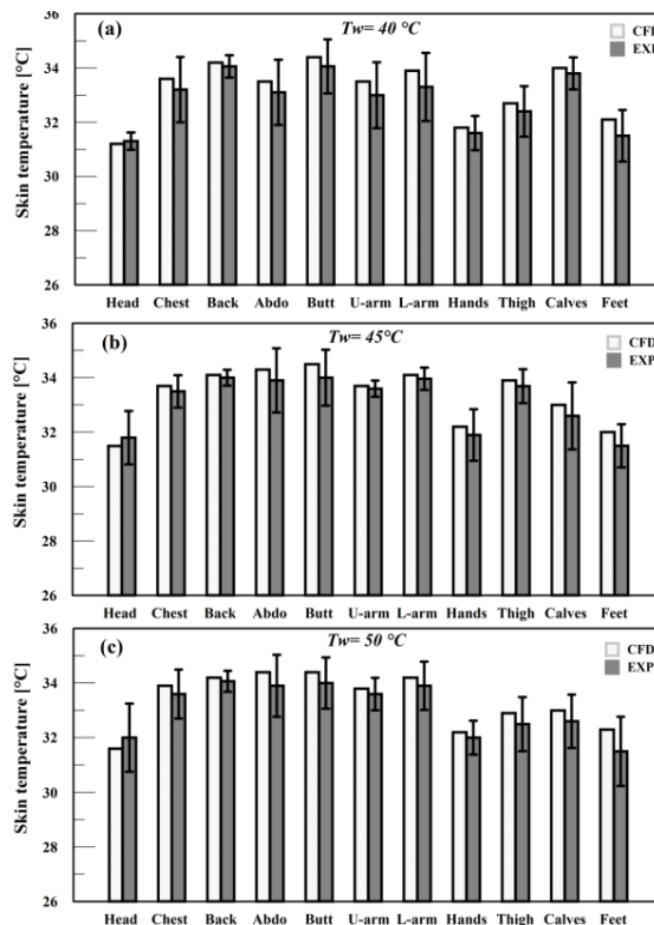**4.1 Experimental Validation of the CFD Model**

To be able to validate the effect of radiation asymmetry caused by a hot window and thermal comfort obtained by operating the proposed PV system, it is important that numerical computations results match the experimental measurements. The numerical model was modified: the diffuse radiation effect was disabled and only long wave radiation due to a hot surface window was investigated experimentally. The panels' boundary conditions were set to a fixed temperature. All other models and boundary conditions were kept the same as the ones used for the parametric study. This computational domain was only used to validate the effect of radiation asymmetry caused by a hot surface and the temperature field variation at the vicinity of the manikin against those measured experimentally. A velocity inflow condition was applied at the boundary of the nozzles and diffuser with a pre-defined temperature as described above while a pressure outlet condition with zero gage pressure was imposed at the return vents. The turbulent intensities obtained from experimental measurements were used as inlet boundary conditions for the CFD simulations: 3% for the nozzle jet and 2% for the diffusers [14,15].

Since radiation asymmetry is simulated in non-homogeneous space, it was necessary to validate the predicted results with an experimental setup and make sure that the coupling between the bioheat and the CFD model is successfully capturing radiation

asymmetry effect on the human body and the localized environment. Measurements of segmental skin temperatures and air temperature at the vicinity of the manikin (in a region limited by a 5cm offset distance from body segment surface) were performed and compared to the predicted temperature values obtained through numerical simulations at $T_w$= 40 °C, $T_w$= 45 °C, and $T_w$= 50 °C. The skin temperature validation served to check for local comfort and thermal draft near sensitive body segments, while the air temperature validation aided to check for thermal field variation at the vicinity of the manikin in asymmetrical environment.

According to Fig. 5(a-c), the lowest air temperature was recorded near the head since it is the first part of the manikin being hit by the cold (16 °C) PV jet, and the highest air temperature was measured near the hands, calves and feet. As a result, the local skin temperature was affected and varied accordingly as depicted in Fig. 6(a-c). For example, when the near head temperature attained the lowest value of 24.3 °C, the head skin temperature reached a minimum value of 32.5 °C and perceived a relatively cold sensation as shown in Fig. 5a and Fig. 6a respectively. As the panels 'surface temperature increases, the skin and air temperature at the vicinity of the manikin kept the same trend but with an upward shift in the values more pronounced at the exposed body segments such as head chest and hands. For example, when the panels' surface temperature increases from 40 °C to 50 °C, the near head air temperature increases by nearly 1.5 °C and the corresponding skin temperature shifted up by 0.5 °C. However, the back, buttocks and feet skin and air temperatures have slightly changed. These observations can be explained due to view factor effect between the panels and manikin body parts in addition to the convection heat transfer phenomena from the hot surface. It

26

is noticed that the numerical model was able to accurately predict the skin and air temperatures since the relative error remained between 3 to 4% for the three different panels' temperatures. The highest error was detected at the head; it can be explained by the lumped approach entailed in the bioheat model for the head body part, while the manikin software divides the head into two thermal zones: forehead and back head. The lowest error was depicted at the back and buttocks (less than 1 or 2 %). The agreement in the results showed that 1- the CFD model is a valid model to examine thermal fields variation due to longwave radiation exchange between surfaces and 2- the mesh can be used to conduct a parametric study.



**Fig. 5 Experimental validation of segmental skin temperature at (a) Tw= 40°C, (b) Tw= 40°C, and (c) Tw= 50 °C.**
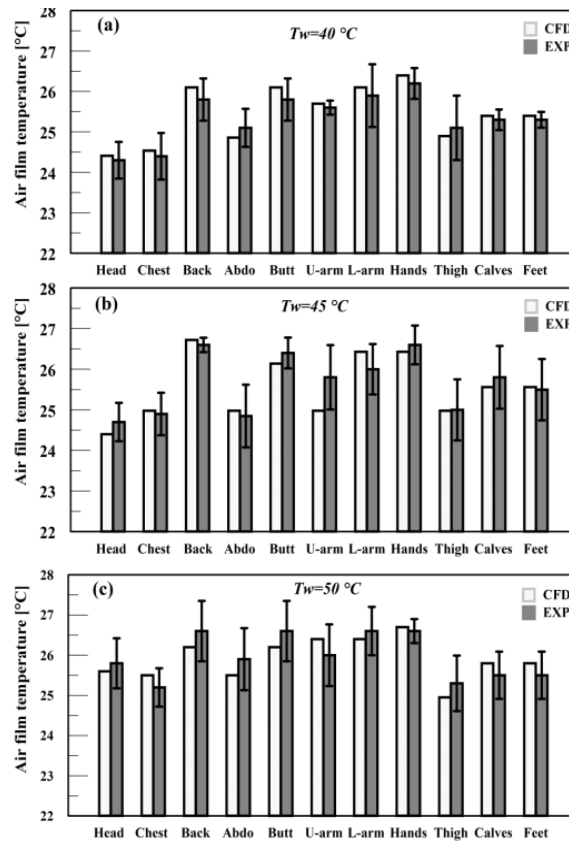
**Fig. 6 Experimental validation of air temperature at the vicinity of each body segment at (a) Tw= 40°C, (b) Tw= 40°C, and (c) Tw= 50 °C.**

## 4.2 Parametric Study

When evaluating the ability of a PV system in providing occupants with desirable thermal comfort in asymmetrical environment, it is crucial to assess local and overall thermal sensation and comfort when using different glazing systems. Extensive simulations were done for 4 different window types. For each glazing system, we varied the peripheral diffuser flow rate between 50 L/s and 55 L/s, and the return air temperature between 19 °C, 18 °C and 16 °C; the optimal operating conditions were selected until an acceptable thermal sensation and comfort were attained with the minimum thermal draft. Comfort zone is defined such as the whole body is comfortable

and there is no local discomfort [16-18]. The 9-point sensation scale ranged from very cold (-4) to very hot (4) and the 9-point comfort scale ranged from very uncomfortable (-4) to very comfortable (4), with 0 representing the transition from discomfort to comfort [17-20]. If thermal comfort cannot be reached at these conditions, the peripheral diffuser flow rate was increased to 60 L/s. In the parametric study, we did not exceed a temperature lower than 16 °C and a flow rate higher than 60 L/s in order to prevent thermal draft sensation and high cooling loads. The primary nozzle operating parameters were fixed for all simulation cases: fresh airflow rate supply of 8.5 L/s (as recommended by ASHRAE [23]) and temperature supply of 16 °C. To compare the energy consumption and comfort preferences at optimal coaxial PV conditions, the analysis has started with high performance window then moving to low performance window. In order to check for thermal draft, the near head velocity and temperature were recorded for each case. Other predicted parameters such as: interior window surface temperature, macroclimate temperature, absorbed diffuse heat flux and segmental net radiative heat flux were predicted for the different glazing systems in order to assess human thermal comfort.

Glazing system G4: When using advanced glazing properties, a desirable overall thermal comfort (1.58) and sensation (0.18) were attained for a diffuser flow rate of 55 L/s and a return air temperature of 19 °C. At these operating conditions, the average room macroclimate temperature (see table 3) and the interior window surface temperature (averaged value over the window surface area) attained a value of 28 °C and 37 °C respectively. The person did not perceive any thermal draft since the near head velocity and temperature were desirable (0.71 m/s and 25.7 °C respectively). The

29

local sensation perceived by the head was -0.98 with a corresponding local comfort of 1.3 as shown in Fig. 7d. The human body tolerance to higher return air temperature can be justified due to a reduced transmitted diffuse radiation falling on each part (6.33 W/m2 on each part) and higher local radiation heat flux coming out of the body as seen in Fig. 8d.

Glazing system G3: G3 has a higher solar transmittance than G4 however a similar interior surface temperature (37.6 °C) is predicted due to relatively equal solar absorptivity and thermal conductivity. The human body showed preference to lower return air temperature of 18 °C and same air flow rate of 55 L/s, at which an approximate macroclimate temperature of 28 °C and transmitted radiation falling on the body up to 8.98 W/m2 were attained (see Table 3). The overall comfort and sensation perceived were 1.46 and -0.04 respectively. However when compared to G4, the thermal draft sensation near the head has slightly increased due to higher velocity (0.73 m/s) and lower temperature (25.61 °C) depicted near the head (see Table 3). Consequently, a local cold sensation of -1.12 with a local comfort of 1.1 was predicted for the head and a lower degree of segmental comfort is depicted with g3 as shown in Fig. 7c.

Glazing system G2: An acceptable overall comfort of 1.42 and a sensation of -0.18 were achieved at a 16 °C return air temperature and 50 L/s supply flow rate. The near head temperature and velocity were found to be 25.32 °C and 0.86 m/s respectively. As a result, the head feels colder (-1.2) and less comfortable (0.96) when compared to G3 and G4 due to higher thermal draft existing near the head. The head skin temperature was increased as shown in Fig. 9b. At these conditions, the predicted interior surface

temperature of G2 was 37 °C. It is important to note that for a return air temperature higher than 16 °C, the comfort dropped due to a warm sensation perceived by the hands, arms and calves. The cooling load must be raised in order to remove the discomfort generated by the radiation falling on the body (se Fig. 8b) and warming the air surrounding the occupant.

Glazing system G1: When G1 is installed, a maximum interior window surface temperature of 41.2 °C and a transmitted diffuse radiation falling on the manikin (14.03 W/m2 for each body part) were expected. The net radiative heat flux coming into the human body increases significantly specially for the body segments directly facing the window as seen in Fig. 8a. Thus, the environment surrounding the occupant gets warmer and radiation asymmetry induces local discomfort. As a result, the occupant preferred a low return air temperature of 16 °C with higher diffuser flow rate up to 60 L/s. The overall comfort attained at this level was 1.25 with a slightly warm sensation of 0.32 perceived by the whole body. The near head temperature was increased to 25.92 °C with a relatively high velocity of 0.9 m/s as presented in Table 3. The perceived sensation was raised to -0.82 for the head and up to 0.85, 0.75 and 0.61 for the hands, lowers arms and calves respectively as shown in Fig. 7a. The human body demonstrates higher skin temperature for these body segments and lower degree of local and overall comfort (see Fig. 9a and 7a).
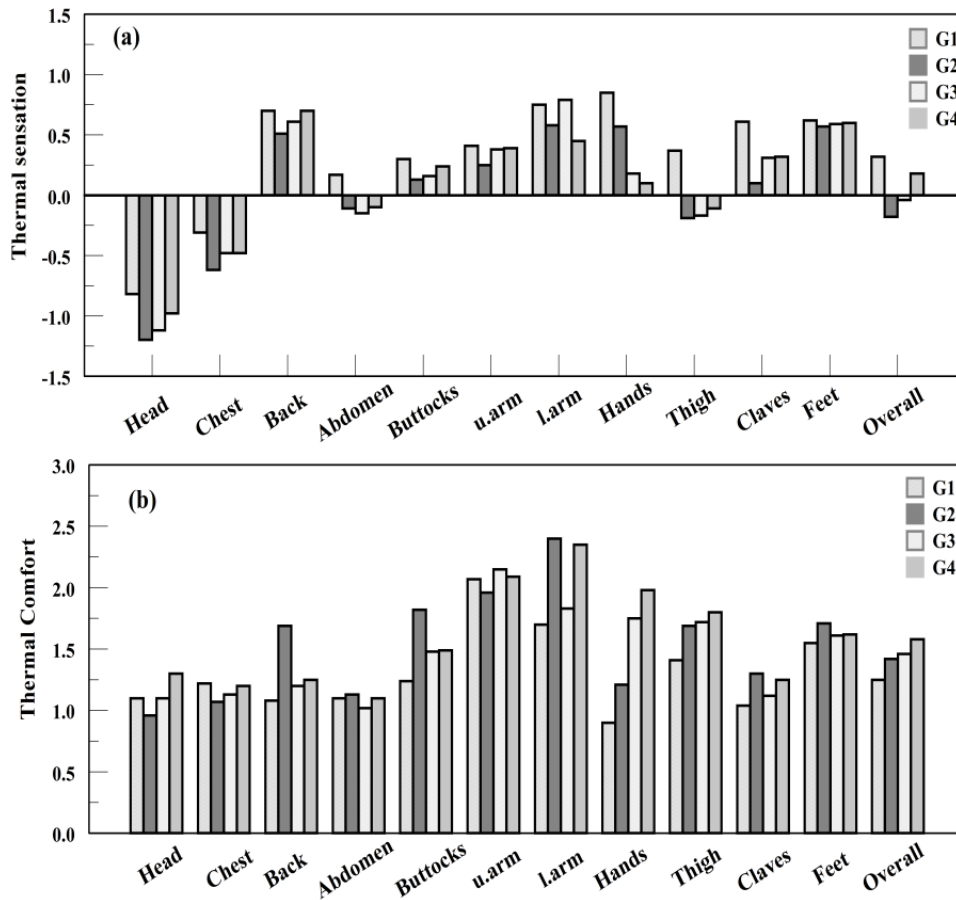
**Fig. 7 Overall and local (a) thermal sensation and (b) thermal comfort attained for the four glazing systems.**

**Table 3**

 **Comparison of near head temperature and velocity, macroclimate temperature and segmental shortwave radiation falling on the body attained with the four glazing systems.**

| Glazing system code | (Diffuser total flow rate, Return air temperature) | Near head temperature [°C] | Near head velocity [m/s] | Macroclimate temperature [°C] | Local absorbed shortwave rad. [W/m$^2$] |
|---|---|---|---|---|---|
| G1 | (60L/s, 16°C) | 25.92 | 0.9 | 28.3 | 14.04 |
| G2 | (50L/s, 16°C) | 25.32 | 0.86 | 28 | 11.78 |
| G3 | (55L/s, 18°C) | 25.61 | 0.73 | 28.2 | 8.98 |
| G4 | (55L/s, 19°C) | 25.35 | 0.71 | 28 | 6.33 |

To sum up, thermal comfort and temperature fields inside the domain are highly influenced by the window inside surface temperature and the transmitted solar radiation, both of which are heavily affected by the glazing properties and the exterior conditions. In other words, the inside surface temperature of the window can significantly affect the radiant heat exchange between an occupant and the surroundings and create discomfort if it becomes greater than the acceptable value [1]. In addition, the transmitted diffuse radiation will be uniformly distributed thus increasing the local sensation of all body parts to a similar degree and resulting in an overall warm sensation [26]. When the thermal properties of the glazed surface improve, the total heat gain decreases and the amount of radiation (longwave and shortwave) absorbed by the body reduces. As a

result, higher supply temperature and/or lower supply flow rate of the coaxial PV system can be used when installing advanced glazing systems (like G4) in order to attain a desirable overall comfort with the optimal degree of segmental comfort of an occupant sitting close to a window. On the contrary, for low performance windows, radiation effect becomes influential on sensitive body parts, and therefore the occupant starts to feel uncomfortable. The discomfort can be triggered by a segmental warm sensation (more pronounced at the hands, calves and back) due to higher total heat load and unpleasant macroclimate temperature. Lowering the temperature or increasing the velocity of the air surrounding the occupant should compensate the impact of low performance window on thermal comfort. However, reducing the cooling set point to offset the room air temperature requires higher energy consumption and might cause thermal draft.
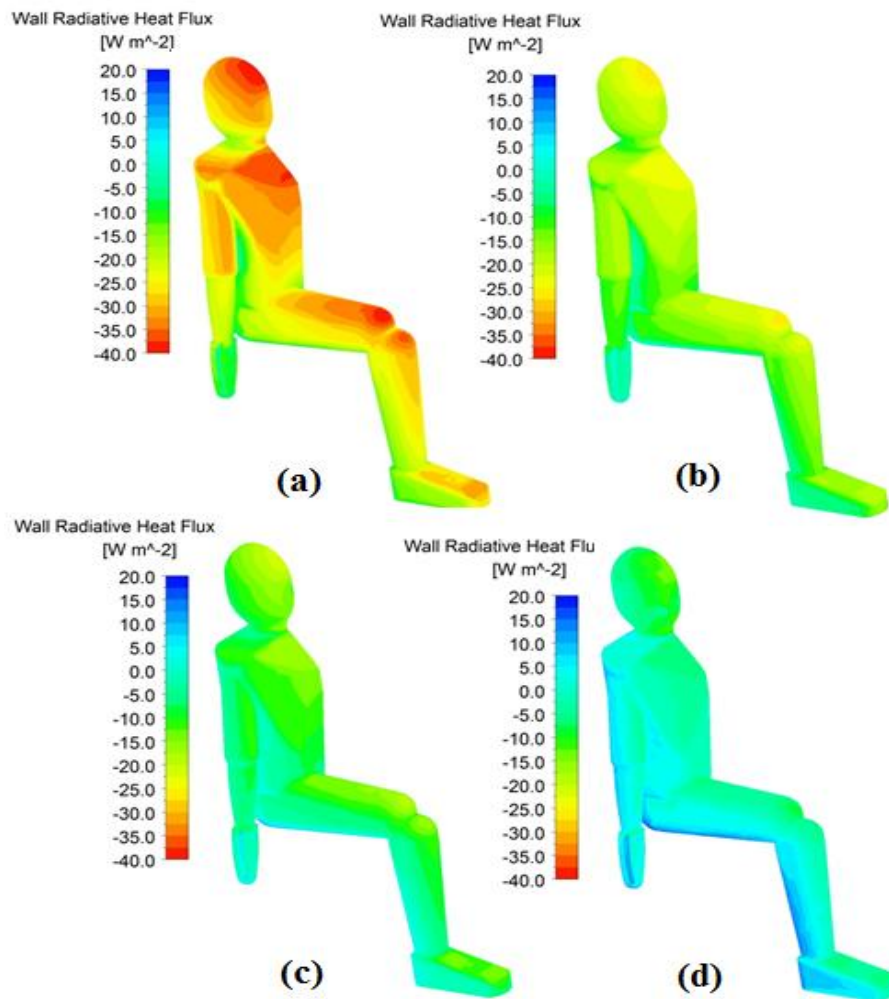
**Fig. 8 Radiative heat flux variation on the manikin body parts at thermal comfort level for (a) G1, (b) G2, (c) G3 and (d) G4. (Positive radiative flux represents a heat loss and a negative value represents a heat gain)**
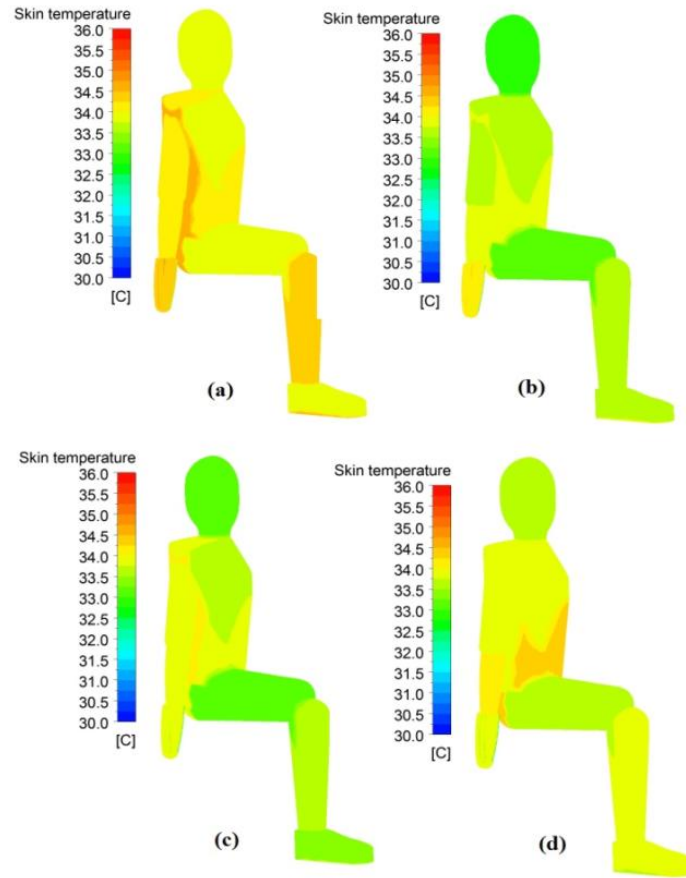
**Fig. 9 Skin temperature distribution at thermal comfort level for (a) G1, (b) G2, (c) G3 and (d) G4.**
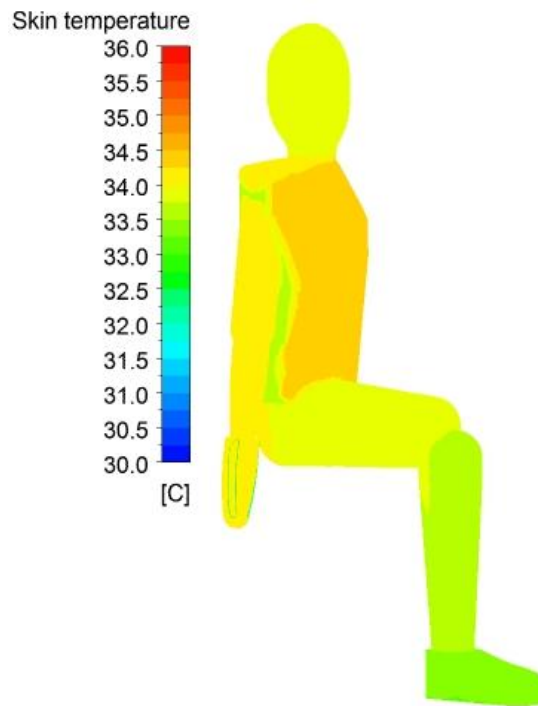
**Fig. 10 Skin temperature distribution for the mixing system case**

## 4.3 Energy Analysis

The main advantage of the personalized ventilation system is its ability to provide thermal comfort for a person sitting close to a window and exposed to asymmetrical conditions caused by the radiation effect. In other words, coaxial PV system can alleviate the thermal tension by localizing cool air motion in order to reduce local discomfort and energy cost. These characteristics of the coaxial system imply a high energy saving potential when compared to conventional mixing system that consists of ceiling diffusers supplying mixed air and controlling the room at a homogeneous air temperature. To be able to create a comfort zone, the PV operating parameters were varied according to the glazing properties, which resulted in different energy

consumptions corresponding to each window type. The cooling load of the PV system was first calculated and compared between the four glazing systems. A chiller COP of 3.5 and a varying fan power used to supply the ceiling-mounted nozzles were assumed to obtain the electrical loads needed to calculate the total electrical energy consumption. According to Table 3, the minimum cooling load of 1.117 KW was achieved with high performance window G4. As the glazing performance degrades, the cooling load increases in order to be able to extract the heat gain coming through the glass and offset the effect of radiation on human comfort. For instance, the cooling load has increased to 1.462 KW, 0.35 KW more energy consumption than G4. Consequently, the best degree of local and overall comfort and energy savings were attained with G4. Whereas with G3, the overall and local comfort were desirable however higher energy consumption is required to remove the heat load. As with G2 and G1, thermal comfort was not totally attainable due to local warm sensation perceived by the lower body parts exposed to radiation effect and the thermal draft perceived by the head.

On the other hand, it would important to compare the energy performance of the coaxial PV system with conventional mixing systems. The energy analysis was done for the same total heat gain using the high performance window G4 and an equal amount of fresh air flow rate (8.5L/s) delivered to the workspace. A maximum total flow rate of 80.5 L/s was fixed for the mixing system, while the supply temperature was varied until reaching an acceptable level of thermal comfort similarly attained with the PV. After running multiple CFD simulations for the mixing case, an overall thermal comfort of 1.1 and a sensation of 0.4 were attained for a supply air temperature of 10 °C and a corresponding average space temperature reached a value of 23.5 °C. The mixed

ventilation room temperature should be low enough to compensate for the uncomfortable warm sensation perceived by sensitive body parts. The skin temperature distribution was relatively higher for the head, chest and thighs when compared to the personalized ventilator as shown in Fig.9. The human body felt comfortable, although lower degree of segmental comfort (more pronounced at the head) was perceived when compared to the PV system. The cool air is no longer localized over these sensitive body segments exposed to radiation asymmetry, thus they perceive a warmer sensation resulting with higher skin temperature. Remarkable energy savings up to 35% were achieved when compared to conventional mixing system.

The energy savings do not depend only on the supply temperature but also on the fresh air amount delivered. In our analysis, same amount of fresh air was used since IAQ was not investigated. However, Makhoul proved that higher amount of fresh air is required to deliver with mixing systems in order to achieve equal level of IAQ attained with the coaxial PV system [14, 15]. It is essential to note that for lower performance window, it is not practical to use mixing ventilation system since it requires high energy consumption to attain a desirable homogeneous temperature capable to offset the radiation effect from the window. In addition, it would be interesting to investigate the payback period of the system since the initial costs of the different glazing greatly differ. However the analysis in this study was done over one hour during a peak summer season, whereas the operating conditions and electrical consumption can vary significantly between each hour, day, month etc.

**Table 4**

**Overall thermal comfort and sensation and the corresponding PV cooling load predicted for the four different glazing systems.**

| Glazing system code | (Diffuser total flow rate, Return air temperature) | Thermal comfort | Thermal sensation | Coaxial Cooling [KWatts] | PV Load |
|---|---|---|---|---|---|
| G1 | (60L/s, 16°C) | 1.20 | 0.32 | 1.462 | |
| G2 | (50L/s, 16°C) | 1.42 | -0.18 | 1.387 | |
| G3 | (55L/s, 18°C) | 1.46 | -0.04 | 1.207 | |
| G4 | (55L/s, 20°C) | 1.58 | 0.15 | 1.117 | |

# CHAPTER 5

# CONCLUSION

The performance of coaxial PV system combined with different glazing systems, ranging from low to high performance, was studied numerically. A radiation model was integrated with the numerical CFD model to account for both longwave radiation between surfaces and shortwave radiation (diffuse only) passing through the window and falling on the human body. Local and overall comfort and sensation of the occupant were assessed in each case since radiation asymmetry and thermal draft are major factors that can create discomfort in non-uniform spaces. The proposed PV system was capable to provide a desirable thermal comfort in asymmetrical environment where large glazing facades are installed and occupant is seated 1 m away from the window. The ability of the integrated system to localize the cool air and create a canopy around the occupant helped mitigate the thermal tension and the uncomfortable warm sensation perceived by the occupant (especially by the head) due to the radiative asymmetrical field.  The impact of low performance window on thermal comfort should be compensated by lowering the air temperature or increasing the air flow rate. However, reducing the cooling set point to offset the room air temperature and induce air motion requires higher energy consumption and causes thermal draft.

The optimal thermal comfort with the minimum energy consumption was predicted when coaxial PV system is combined with high performance window like G4. When compared to conventional mixing system, the coaxial PV system showed a high energy savings up to 35% potential. Finally, in harsh summer conditions, it is not practical to

use low performance window with mixing systems. The use of high performance window can reduce human discomfort caused by radiation effect; however it is not energy efficient when combined with mixing systems. Localized air conditioning systems such as the coaxial PV systems are more energy efficient and feasible to use in asymmetrical environment since they deliver cool fresh air directly to the breathing zone and reduce thermal tension in the workspace.

# BIBLIOGRAPHY

[1] C. Huizenga, H. Zhang, P. Mattelaer, T. Yu, E.A. Arens, P. Lyons. Window performance for human thermal comfort. Final report to the national fenestration rating council, center for the built environment, (2006)

[2] P.R.A. Lyons, D. Arasteh, C. Huizenga. Window Performance for Human Thermal Comfort. ASHRAE Transactions 73 (2) (1999), pp. 4.0 – 4.20

[3] K. Tsikaloudaki, T. Theodosiou, K. Laskos, D. Bikas. Assessing cooling energy performance of windows for residential buildings in the Mediterranean zone. Energy Build, 64 (2012), pp. 335-343

[4] R.-L. Hwang, S.-Y. Shu. Building envelope regulations on thermal comfort in glass façade buildings and energy-saving potential for PMV based comfort control. Build. Environ., 46(2011), pp. 824-834.

[5] F. Cappelletti, A. Prada, P. Romagnoni, A. Gasparella. Passive performance of glazed components in heating and cooling of an open-space office under controlled indoor thermal comfort. Build. Environ., 72 (2014), pp. 131-144

[6] L. Zhang, T. Chow, K. Fong, Q. Wang, Y. Li. Comparison of performances of displacement and mixing ventilations. Part I: thermal comfort. Int J Refrigeration. 28(2) (2005):276e87.

[7] L. Zhang, T. Chow, K. Fong, C. Tsang, Q. Wang. Comparison of performances of displacement and mixing ventilations. Part II: indoor air quality. Int J Refrigeration, 28(2) (2005):288e305.

[8]L. Zhang, C. Lee, S. Fong, T. Chow, T. Yao, A. Chan, Comparison of annual energy performances with different ventilation methods for cooling. Energy Build., 43(1) (2001):130e6.

[9]L. Zhang, C. Lee, K. Fong, T. Chow. Comparison of annual energy performances with different ventilation methods for temperature and humidity control. Energy Build., 43(12) (2011):3599e608

[10]   B. Halvonova, A. Melikov, Performance of "ductless" personalized ventilation in conjunction with displacement ventilation: Impact of intake height. Building and Environment 45(4) (2010):996e1005.

[11]   R. Li, S. Sekhar, A. Melikov, Thermal comfort and IAQ assessment of under-floor air distribution system integrated with personalized ventilation in hot and humid climate. Building and Environment 45(9) (2010):1906e13.

[12]   B. Yang, Thermal comfort and indoor air quality evaluation of a ceiling mounted personalized ventilation system integrated with an ambient mixing ventilation system. PhD thesis, National University of Singapore, (2009).

[13]   B. Yang, S. Chandra, A. Melikov, Ceiling mounted personalized ventilation system in hot and humid climate - an energy analysis. Energy and Buildings 42 (2010): 2304e8.

[14]   A. Makhoul, K. Ghali, N. Ghaddar. Ceiling-Mounted Fresh Air Personalized Ventilator System for Occupant-Controlled Microenvironment. In ASME 2012 International Mechanical Engineering Congress and Exposition, American Society of Mechanical Engineers, (2012), pp. 1683-1693

[15]   A. Makhoul, K. Ghali, N. Ghaddar. Thermal comfort and energy performance of a low-mixing ceiling-mounted personalized ventilator system. Build. Environ., 60(2013), 126-136.

[16]   Salloum M, Ghaddar N, Ghali K. A new transient bioheat model of the human body and its integration to clothing models. Int J Thermal Sci 2007; 46:371e84.

[17]   Zhang H, Arens E, Kim D, BuchBerger E, Bauman F, Huizanga C. Comfort, perceived air quality, and work performance in a low-power task ambient conditioning system. Build. Environ., 45(1) (2010):29e39

[18]   Zhang H, Arens E, Huizenga C, Han T. Thermal sensation and comfort models for non-uniform and transient environments: Part I: local sensation of individual body parts. Build. Environ., 45(2) (2010):380e8.

[19]   Zhang H, Arens E, Huizenga C, Han T. Thermal sensation and comfort models for non-uniform and transient environments: Part II: local comfort of individual body parts. Build. Environ., 45(2) (2010):389e98.


[20]   Zhang H, Arens E, Huizenga C, Han T. Thermal sensation and comfort models for non-uniform and transient environments: Part III: whole-body sensation and comfort. Build. Environ., 45(2) (2010):399e410.

[21]   W. Chakroun, N. Ghaddar, K. Ghali. Chilled ceiling and displacement ventilation aided with personalized evaporative cooler: thermal comfort and energy savings. Energ. Build., 43(11) (2011):3250e7.

[22]    N. Ghaddar, K. Ghali, S. Chehaitly. Assessing thermal comfort of active people in transitional spaces in presence of air movement. Energ. Build., 43(10) (2011):2832e42.

[23]    ASHRAE. ANSI/ASHRAE standard 621-2013, Ventilation for Acceptable Indoor Air Quality. Atlanta: American Society of Heating, Air-Conditioning and Refrigeration Engineers, Inc.; 13

[24]    ANSYS Software. ANSYS Inc.  http://www.ansys.com/.

[25]    Fluent, ANSYS (2009). 12.0 Theory Guide. *Ansys Inc*, *5*.

[26]    S. Hoffmann, C. Jedek, E. Arens. Assessing thermal comfort near glass facades with new tools. In BEST 3 Building Enclosure Science and Technology Conference, (2012)

[27]    B.W. Olesen, K.C. Parsons. Introduction to thermal comfort standards and to the proposed new version of EN ISO 7730. Energy Build., 34(6) (2002)

[28]    S. Hussain, P. Oosthuizen. Numerical study of the effect of atrium design changes on the flow rate and temperature distributions in a simple atrium building and thermal comfort evaluation, Applied Thermal Engineering, 40  (2012): 358e372.

[29]    S. Hussain, P. Oosthuizen. Numerical investigations of buoyancy-driven natural ventilation in a simple three-storey atrium building and thermal comfort evaluation. Applied Thermal Engineering, 57(1) (2013), pp. 133-146.

[30]    G. Sevilgen, M. Kiliç. Investigation of transient cooling of an automobile cabin with a virtual manikin under solar radiation. Thermal Science, 17(2) (2013), pp. 397-406.

[31]    M. Kilic, G. Sevilgen. Modeling airflow, heat transfer and moisture transport around a standing human body by computational fluid dynamics. International Communications in Heat and Mass Transfer, 35(9) (2008), pp. 1159-1164.

[32]    R. Mitchell, C. Kohler, D.  Curcija, L. Zhu, S. Vidanovic, S. Czarnecki, D. Arasteh. THERM 6.3/WINDOW 6.3 NFRC simulation manual. Lawrence Berkeley National Laboratory, (2013):48255.

[33]    Li B, Li W, Liu H, Yao R, Tan M, Jing S and Ma X. Physiological Expression of Human Thermal Comfort to Indoor Operative Temperature in the Non-HVAC Environment. Indoor Built Environ, 19(2) (2010), pp. 221-229.

[34]    Epoxy Thermal Manikin. INSTRUMENTS FOR TEXTILE & BIOPHYSICAL TESTING.        Seattle,        WA,        [Online].        Available: http://www.thermetrics.com/sites/default/files/product_brochures/NEWTON%20Manikin_Spec%20Sheet.pdf

[35]    A. Hassan, N. Hejase, A.H. Assi. Global and Diffuse Solar Radiation in the United Arab Emirates. International Journal of Environmental Science and Development, 4(5) (2013) 470-474.

[36]    J.A. Palyvos, A survey of wind convection coefficient correlations for building envelope energy systems, modeling. Applied and Thermal Engineering, 28 (2008):801e810.